Four-Step Evolution of Spin-Hall Conductance: Tight-Binding Electrons with Rashba Coupling in a Magnetic Field

Yi-Fei Wang[1], Yang Zhao[1], and Chang-De Gong[2,1]
[1]*National Laboratory of Solid State Microstructures and Department of Physics, Nanjing University, Nanjing 210093, China*
[2]*Department of Physics, Suzhou University, Suzhou 215006, China*
(Dated: February 2, 2008)

An intriguing magneto-transport property is demonstrated by tight-binding lattice electrons with Rashba spin-orbit coupling (SOC) in a magnetic field. With the flux strength $\phi = 2\pi/N$ (N is an integer) and the Zeeman splitting fixed, when increasing the Rashba SOC λ, the spin-Hall and charge-Hall conductances (SHC and CHC) undergo four-step evolutions: the SHC shows size-dependent resonances and jumps at three critical λ_c's, and changes its sign at λ_{c1} and λ_{c3}; while the CHC exhibits three quantum jumps by $-Ne^2/h$, $+2Ne^2/h$ and $-Ne^2/h$. Such four-step evolutions are also reflected in topological characters and spin polarizations of edge states of a cylindrical system, and are robust against weak disorder.

PACS numbers: 72.25.-b, 71.70.Ej, 73.43.Cd, 71.10.Ca

Introduction.—Recently, the spin-Hall effect (SHE), i.e., a generation of spin current perpendicular to an applied electric field [1, 2, 3, 4], has shed new light on spintronics [5] and provided novel techniques to manipulate spins in nanostructures. In contrast to the extrinsic SHE driven by spin-orbit (SO) impurity scattering [1], it is proposed that an intrinsic SHE exist in semiconductors with SO coupled bands [2, 3]. These proposals encouraged the discovery of the SHE in GaAs semiconductor films and heterostructures [4], and in metallic Al films and Pt strips [6]. In models with SO coupled bands, two-dimensional electron gas (2DEG) with Rashba spin-orbit coupling (SOC) [7] has the simplest form and is therefore most notable [3, 8, 9, 10, 11]. Meanwhile, tunable Rashba SOC has been achieved via an external gate voltage on the top of asymmetric heterostructures [12], and the Rashba SO field in quantum wells and semiconductors can also be measured optically [13].

In a clean 2DEG with parabolic dispersion and linear Rashba SOC, Sinova *et al.* predicted that the spin-Hall conductance (SHC) holds a universal value independent of SOC strength when both SO split bands are occupied [3]. It is now known that such an intrinsic SHC with only linear Rashba SOC might be destroyed by any amount of disorder [10], or be canceled completely by intrabranch contributions in the presence of a magnetic flux [8]. In parallel, the SHC of 2DEG with linear Rashba SOC and Zeeman splitting in a magnetic field was calculated, and a resonant SHC was predicted when two Landau levels cross each other at the Fermi level [11].

In the presence of an underlying lattice potential, e.g. in metallic conductors like Al films and Pt strips [6], both parabolic dispersion and linear SOC should be modified and then incorporated into a lattice model which has been employed to study the effect of disorder on the SHE in the metallic regime [9]. Here, we begin to investigate a lattice system of 2D tight-binding electrons (TBE) with Rashba SOC in a magnetic field. This model is also relevant to novel experimental systems such as untracold fermions in an optical lattice with an effective SOC [14] and graphene with an intrinsic or Rashba SOC [15, 16]. We focus on magneto-transport properties, and have found that tuning the Rashba SOC strength generates novel four-step evolutions of the SHC and the charge-Hall conductance (CHC). Such bulk properties are also reflected in topological characters and spin polarizations of edge states of a cylindrical system, and are robust against weak disorder.

Formulation.—The model Hamiltonian of 2D TBE on a square lattice with Rashba SOC and a uniform perpendicular magnetic field $\vec{B} = (0, 0, -B)$ is [9]:

$$H = -t\sum_{\langle ij\rangle}\left[e^{i\phi_{ij}}\hat{c}_i^\dagger \hat{c}_j + \text{H.c.}\right] + \lambda\sum_i\left[ie^{i\phi_{i,i+\vec{y}}}\hat{c}_i^\dagger\sigma_x\hat{c}_{i+\vec{y}} - ie^{i\phi_{i,i+\vec{x}}}\hat{c}_i^\dagger\sigma_y\hat{c}_{i+\vec{x}} + \text{H.c.}\right] - h_z\sum_i(n_{i\uparrow} - n_{i\downarrow}) \quad (1)$$

where $\hat{c}_i^\dagger = (c_{i\uparrow}^\dagger, c_{i\downarrow}^\dagger)$ are electron creation operators at site i, σ_x and σ_y are Pauli matrices, the nearest-neighbor hopping integral t will be taken as the unit of energy, λ is the Rashba SOC strength, and the Zeeman splitting parameter is $h_z = \frac{1}{2}g\mu_b B$ with g the Landé factor and μ_b the Bohr magneton. The magnetic flux per plaquette is $\phi = \sum_\square \phi_{ij} = 2\pi Ba^2/\phi_0 = 2\pi/N$ with N an integer, a the lattice constant and $\phi_0 = hc/e$ the flux quantum. The Landau gauge $\vec{A} = (0, -Bx, 0)$ and the corresponding periodical boundary conditions (PBCs) are adopted, and the magnetic unit cell has the size $N \times 1$.

After the numerical diagonalization of the Hamiltonian [Eq. (1)], the zero-temperature ($T = 0$) CHC is calculated through the Kubo formula [17]

$$\sigma_{\text{CH}}(E) = \frac{ie^2\hbar}{A}\sum_{\varepsilon_{m\mathbf{k}}<E}\sum_{\varepsilon_{n\mathbf{k}}>E} \frac{\langle m\mathbf{k}|v_x|n\mathbf{k}\rangle\langle n\mathbf{k}|v_y|m\mathbf{k}\rangle - \langle m\mathbf{k}|v_y|n\mathbf{k}\rangle\langle n\mathbf{k}|v_x|m\mathbf{k}\rangle}{(\varepsilon_{m\mathbf{k}} - \varepsilon_{n\mathbf{k}})^2} \quad (2)$$

while the SHC at $T=0$ is given by [3]

$$\sigma_{\rm SH}(E) = -\frac{e\hbar}{A}\sum_{\varepsilon_{m\mathbf{k}}<E}\sum_{\varepsilon_{n\mathbf{k}}>E}\frac{{\rm Im}\langle m\mathbf{k}|J_x^{z{\rm spin}}|n\mathbf{k}\rangle\langle n\mathbf{k}|v_y|m\mathbf{k}\rangle}{(\varepsilon_{m\mathbf{k}}-\varepsilon_{n\mathbf{k}})^2} \tag{3}$$

where $A = L\times L$ is the area of this 2D system, E is the Fermi energy, $\varepsilon_{m\mathbf{k}}$ is the corresponding eigenvalue of the eigenstate $|m\mathbf{k}\rangle$ of mth Landau subband, and the summation over wave vector $\mathbf{k}$ is restricted to the magnetic Brillouin zone (MBZ): $-\pi/N \le k_x a < \pi/N$ and $-\pi \le k_y a < \pi$. The velocity operator is defined as $\mathbf{v} = i/\hbar[H,\mathbf{R}]$ ($\mathbf{R}$ is the position operator of electron) and the spin current operator as $J_x^{z{\rm spin}} = \hbar/4\{v_x,\sigma_z\}$. When E falling in energy gaps, we can rewrite $\sigma_{\rm CH}$ as $\sigma_{\rm CH}(E) = e^2/h\sum_{\varepsilon_m<E} C_m$, where C_m is the Chern number [17] of the mth totally filled Landau subband.

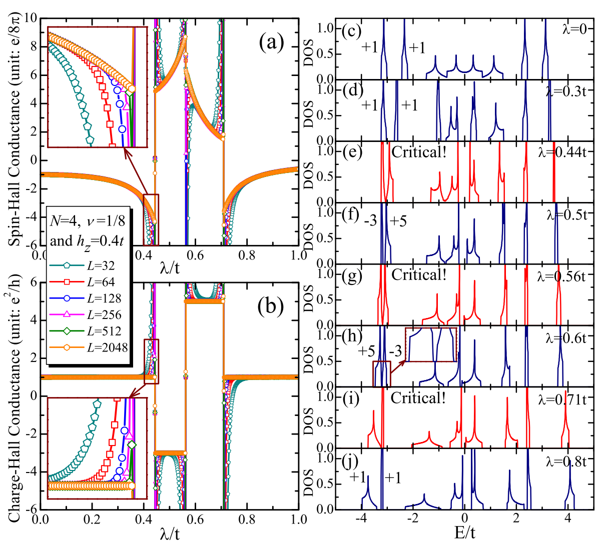

FIG. 1: (color online). The case with $N=4$ and $h=0.4t$. (a) The spin-Hall conductance $\sigma_{\rm SH}$ versus the Rashba SOC parameter λ for electron filling $\nu=\frac{1}{8}$ and various lattice sizes. (b) The charge-Hall conductance $\sigma_{\rm CH}$ versus λ in the cases of (a). (c)-(j) The DOS for some λ's in (a). The Chern numbers of subbands are also shown.

An example with $N=4$.—An overall picture of the CHC $\sigma_{\rm CH}$ and the SHC $\sigma_{\rm SH}$ calculated by Eq. (2) and Eq. (3) are shown in Fig. 1 with $N=4$ (i.e., the flux strength $\phi = \frac{1}{4}\times 2\pi$), $h_z = 0.4t$ and various lattice sizes with $L = 32-2048$. We concentrate on the lowest Landau subbands and consider the electron filling $\nu=\frac{1}{8}$.

In the case of $\lambda = 0$ [Fig. 1(c)], the density of states (DOS) is symmetric about the Fermi energy E, and the lowest two Landau subbands (each totally-filled subband contributes $\frac{1}{8}$ to ν) are well separated, each carrying a Chern number $+1$. With λ increasing from 0 to $1.0t$ one sees a systematic four-step evolution of $\sigma_{\rm CH}$ and $\sigma_{\rm SH}$ versus λ; there are three critical λ_c's at which both $\sigma_{\rm SH}$ and $\sigma_{\rm CH}$ exhibit jumps.

When λ increases from 0 to $\lambda_{c1}\approx 0.44t$, the lowest two Landau subbands approach each other, then merge together and form a pseudogap at λ_{c1} [Fig. 1(e)]; $\sigma_{\rm SH}$ changes continuously from $-1e/8\pi$ to larger negative values [Fig. 1(a)]; while $\sigma_{\rm CH} = +1e^2/h$ nearly stays unchanged [Fig. 1(b)]. Here for a small lattice size ($L=32$), $\sigma_{\rm SH}$ and $\sigma_{\rm CH}$ both present divergence when λ approaches λ_{c1}. With the lattice size increased ($L = 64-512$), the divergence is weakened accordingly; for $L=2048$, $\sigma_{\rm SH}$ approaches a finite value $-4.30e/8\pi$ at λ_{c1}, and $\sigma_{\rm CH}$ remains as $+1e^2/h$ for $0\le\lambda<\lambda_{c1}$. In the following, we focus on the data obtained with $L=2048$.

Increasing λ across each λ_c, $\sigma_{\rm SH}$ and $\sigma_{\rm CH}$ both exhibit sharp jumps: $\sigma_{\rm SH}$ jumps from -4.30 to $+4.87$ (in units of $e/8\pi$) at λ_{c1}, from $+8.71$ to $+6.32$ at $\lambda_{c2}\approx 0.56t$, and from $+1.49$ to -3.57 at $\lambda_{c3}\approx 0.71t$; $\sigma_{\rm CH}$ changes as $+1\to -3\to +5\to +1$ (in units of e^2/h). In intervals away from λ_c's, $\sigma_{\rm SH}$ varies continuously while $\sigma_{\rm CH}$ remains unchanged. The corresponding DOS [Fig. 1(c-j)] also points out that the lowest two Landau subbands approach, merge together and form a pseudogap at each λ_c, and then separate for three times.

Mainly, such a four-step evolution of the SHC of TBE is distinct from the resonant SHC of 2DEG predicted by Shen *et al.* [11] in four aspects: in 2DEG, two Landau levels cross each other at the Fermi level only once and produce one λ_c, while for TBE the two Landau subbands touch successively three times and results in three λ_c's; at a λ_c, the SHC of 2DEG diverges at $T=0$, while the SHC of TBE converges to finite values in the thermodynamic limit ($L\to\infty$) at $T=0$; the SHC of 2DEG does not change its sign while the SHC of TBE changes its sign at λ_{c1} and λ_{c3}; furthermore, the CHC of 2DEG is unaffected when tuning λ, but the CHC of TBE presents three successive quantum jumps.

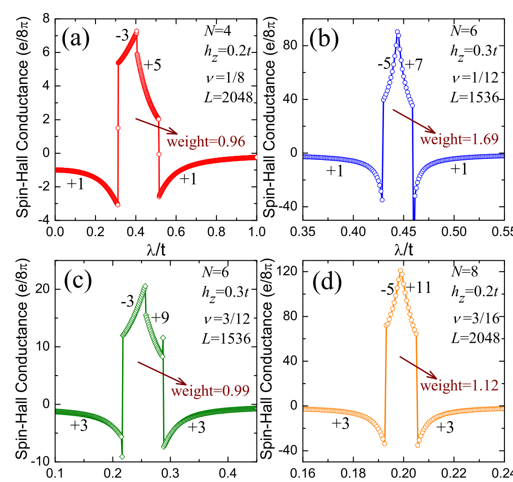

FIG. 2: (color online). $\sigma_{\rm SH}$ versus the Rashba SOC parameter λ in various cases. $\sigma_{\rm CH}$ (in units of e^2/h) of each evolution step is also shown.

Cases with weaker magnetic fields.—The above four-step evolutions have also been verified by further numerical calculations of the cases with $N = 4-16$, $h_z =$

$0.05t - 0.4t$, and various ν's (with odd number of totally filled Landau subbands), as illustrated by four examples in Fig. 2. For $N = 4$, $h_z = 0.2t$ and $\nu = 1/8$ [Fig. 2(a)], $\sigma_{\rm SH}$ shows behaviors similar to that in Fig. 1(a), while with smaller λ_c's and narrower transition regions (i.e., smaller $\lambda_{c3} - \lambda_{c1}$); for $N = 6$ and $N = 8$ [Fig. 2(b-d)], the transition regions are narrower than the case with $N = 4$. Meanwhile, the quantized CHC also exhibits three jumps by $-Ne^2/h$, $+2Ne^2/h$ and $-Ne^2/h$.

In brief, the larger N's, the significantly narrower are the transition regions ($\lambda_{c1} \le \lambda \le \lambda_{c3}$). However, the positive values in the transition regions are much larger, and the total weights of positive part of $\sigma_{\rm SH}$ (i.e. the integral from λ_{c1} to λ_{c3}) possessing the same order of magnitude, are respectively 0.96, 1.69, 0.99 and 1.12 in the four cases of Fig. 2. [Note that the weight is 1.22 for the case in Fig. 1(a).]

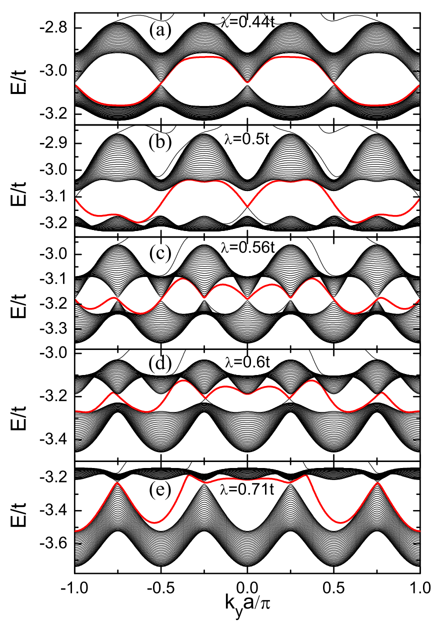

FIG. 3: (color online). Lowest two subbands and intermediate edge states [shown as thick (red) lines] of a cylinder of the size $128 \times \infty$ (OBC in x direction and PBC in y direction) with $N = 4$, $h_z = 0.4$ and various λ's.

Edge states in a cylindrical system with $N = 4$.— An alternative way to reveal the distinctions among four evolution steps is to calculate the edge states of the system on a cylinder. These edge states reflect the topological character of the corresponding bulk state [19, 20]. Just recently, spin-filtered edge states have been considered for a graphene cylinder with an intrinsic SOC [15] (in a two-component Haldane model [21]) or Zeeman splitting [18], a quantum SHE arising from helical edge states have been proposed and experimentally verified soon in HgTe quantum wells [22], and edge states have also been employed to characterize topological band insulators and chiral spin liquids [23]. Now as an illustration, we take a cylinder of square lattice of the size $128 \times \infty$ and apply open boundary condition (OBC) in x direction and PBC in y direction.

Chern numbers of bulk Landau subbands are intimately related to the winding numbers of the corresponding edge states [20]. For $\lambda_{c1} < \lambda < \lambda_{c2}$, there is one edge state winding three times from the upper subband to the lower one then back to the upper one [a thick (red) line in Fig. 3(b)] which corresponds to a Chern number -3 of the lower subband. For $\lambda_{c2} < \lambda < \lambda_{c3}$, there is one edge state winding five times from the lower subband to the upper one then back to the lower one [Fig. 3(d)] which corresponds to a Chern number $+5$ of the lower subband. While for $0 < \lambda < \lambda_{c1}$ or $\lambda_{c3} < \lambda < 1.0t$ (not shown in Fig. 3), there is another edge state winding only once from the lower subband to the upper one then back to the lower one which corresponds to a Chern number $+1$ of the lower subband.

The continuum spectrum of this cylinder also gives further descriptions about the jumps of the bulk CHC. Increasing λ across λ_{c1} [Fig. 3(a)] or λ_{c3} [Fig. 3(e)], the lowest two subbands touch at four points simultaneously in k-space and a Chern number -4 is transfered from the upper subband to the lower one; while across λ_{c2} [Fig. 3(c)], the lowest two subbands touch at eight points simultaneously in k-space and a Chern number $+8$ is transferred between them. Such a correspondence between transferred chern numbers and touching points in k-space has also been verified for $N = 5 - 8$.

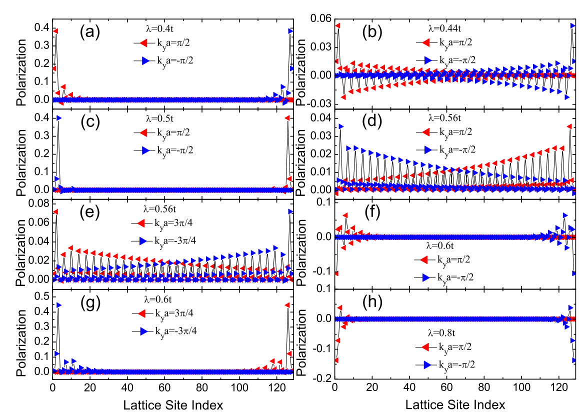

FIG. 4: (color online). Spin polarization P^z (in units of $\hbar/2$) versus the lattice site index in x direction for the edge states of the cylindrical system in Fig. 3.

In addition, the spin polarization carried by the edge states can be computed explicitly as $P^z_{m\mathbf{k}}(i) = \hbar/2\langle m\mathbf{k}|\hat{c}_i^\dagger \sigma_z \hat{c}_i|m\mathbf{k}\rangle$ with i the lattice site index in x direction [16]. In Fig. 4, we plot the spin polarization P^z of some edge states of the above cylindrical system. If λ takes a value far away from λ_c's, P^z takes prominently large values near the left or the right edge and is almost zero in the intermediate region [Fig. 4(a), (c) and (f-h)]; but if λ takes a value close to λ_c's, P^z fluctuates strongly between two edges [Fig. 4(b), (d) and (e)]. Note that for

a fixed k_y, the dominantly positive peak of P^z moves to another edge when λ varies from $0.4t$ to $0.5t$. And for edge states of $\lambda = 0.8t$ [Fig. 4(h)], P^z takes prominently negative values near edges.

Presence of disorder.— We add a term $\sum_i w_i \hat{c}_i^\dagger \hat{c}_i$ [9] into the Hamiltonian [Eq. (1)] to account for the effects of nonmagnetic disorder, w_i being a random potential uniformly distributed between $[-W/2, W/2]$.

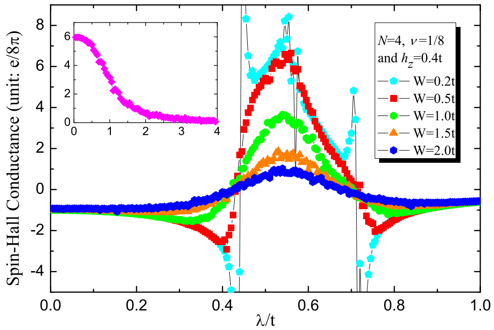

FIG. 5: (color online). σ_{SH} versus λ in the case with $N = 4$, $h_z = 0.4t$ and various disorder strength W's (100 random-potential configurations of the size 8×8). The inset shows the evolution of σ_{SH} versus W at $\lambda = 0.5t$.

For $N = 4$, the adopted 100 random-potential configurations are of the size 8×8 (such a super unit cell is commensurate with the magnetic unit cell in the absence of disorder), and the total lattice is of the size 32×32. It can be seen that weak disorder ($W \leq 0.5t$) does not smear out the overall four-step evolution of the SHC. For stronger disorder ($W = 2.0t$), the SHC does not show resonance anymore near λ_{c1} or λ_{c3}, and takes positive values in an enlarged interval while the peak is diminished into a hump.

Summary and discussion.—An appealing evolution of magneto-transport property has been demonstrated by TBE with Rashba SOC in a magnetic field: (i) with the flux strength $\phi = 2\pi/N$ and the Zeeman splitting fixed, when increasing the Rashba SOC λ from 0, four-step evolutions of the SHC and CHC have been observed; (ii) at three λ_c's, the SHC shows size-dependent resonances and jumps, and changes its sign at λ_{c1} and λ_{c3}; (iii) meanwhile, the quantized CHC shows three successive jumps by $-Ne^2/h$, $+2Ne^2/h$ and $-Ne^2/h$; (iv) for smaller ϕ's, the total weights of positive part of SHC have the same order of magnitude although the transition regions are significantly narrower; (v) edge states of a cylindrical system reflect such bulk properties; (vi) this four-step evolution is robust against weak disorder.

Such a four-step evolution of SHC is expected to occur in 2D electron systems with a lattice potential, a mechanism of SOC or SO scattering, and an external magnetic field. Some candidate experimental systems are: metallic conductors such as Al films and Pt strips [6], untracold fermions in an optical lattice with an effective SOC [14], and graphene with an intrinsic or Rashba SOC [15, 16]. And spin polarizations of edge states should be observable in a four-terminal experimental setup [15, 18].

This work was supported by the National Nature Science Foundation of China (No. 90503014), the State Key Program for Basic Researches of China (No. 2006CB921802), China Postdoctoral Science Foundation (No. 20070410330) and Jiangsu Planned Projects for Postdoctoral Research Funds (No. 0602021C).

[1] M.I. D'yakonov and V.I. Perel', Sov. Phys. JETP Lett. **13**, 467 (1971); J.E. Hirsch, Phys. Rev. Lett. **83**, 1834 (1999); S. Zhang, Phys. Rev. Lett. **85**, 393 (2000).
[2] S. Murakami, N. Nagaosa, and S. C. Zhang, Science **301**, 1348 (2003).
[3] J. Sinova *et al.*, Phys. Rev. Lett. **92**, 126603 (2004).
[4] Y.K. Kato *et al.*, Science **306**, 1910 (2004); J. Wunderlich *et al.*, Phys. Rev. Lett. **94**, 047204 (2005).
[5] S.A. Wolf *et al.*, Science **294**, 1488 (2001); I. Žutić, J. Fabian, and S. Das Sarma, Rev. Mod. Phys. **76**, 323 (2004).
[6] S.O. Valenzuela, M. Tinkham, Nature **442**, 176 (2006); T. Kimura *et al.*, Phys. Rev. Lett. **98**, 156601 (2007).
[7] Y.A. Bychkov and E.I. Rashba, Sov. Phys. JETP Lett. **39**, 78 (1984); J. Phys. C **17**, 6039 (1984).
[8] E.I. Rashba, Phys. Rev. B, 70, 201309(R) (2003).
[9] L. Sheng, D.N. Sheng, and C.S. Ting, Phys. Rev. Lett. **94**, 016602 (2005); D.N. Sheng, L. Sheng, Z.Y. Weng, and F.D.M. Haldane, Phys. Rev. B **72**, 153307 (2005).
[10] H.A. Engel, E.I. Rashba, and B.I. Halperin, arXiv: cond-mat/0603306.
[11] S.Q. Shen, M. Ma, X.C. Xie, and F.C. Zhang, Phys. Rev. Lett. **92**, 256603(2004); F.C. Zhang and S.Q. Shen, arXiv: cond-mat/0703176.
[12] J. Nitta, T. Akazaki, H. Takayanagi, and T. Enoki, Phys. Rev. Lett. **78**, 1335 (1997).
[13] L. Meier *et al.*, Nature Phys. **3**, 650 (2007).
[14] T.D. Stanescu, C. Zhang, and V. Galitski, Phys. Rev. Lett. **99**, 110403 (2007).
[15] C.L. Kane and E.J. Mele, Phys. Rev. Lett. **95**, 146802 (2005); **95**, 226801 (2005).
[16] L. Sheng, D.N. Sheng, C.S. Ting, and F.D.M. Haldane, Phys. Rev. Lett. **95**, 136602 (2005); D.N. Sheng, Z.Y. Weng, L. Sheng, and F.D.M. Haldane, Phys. Rev. Lett. **97**, 036808 (2006).
[17] D.J. Thouless, M. Kohmoto, M.P. Nightingale, and M. den Nijs, Phys. Rev. Lett. **49**, 405 (1982).
[18] D.A. Abanin, P.A. Lee, and L.S. Levitov, Phys. Rev. Lett. **96**, 176803 (2006).
[19] B.I. Halperin, Phys. Rev. B **25**, 2185 (1982).
[20] Y. Hatsugai, Phys. Rev. Lett. **71**, 3697 (1993).
[21] F.D.M. Haldane, Phys. Rev. Lett. **61**, 2015 (1988).
[22] B.A. Bernevig, T.L. Hughes, S.C. Zhang, Science **314**, 1757 (2006); M. König *et al.*, Science **318**, 766 (2007).
[23] D.H. Lee, G.M. Zhang, and T. Xiang, Phys. Rev. Lett. **99**, 196805 (2007); H. Yao and S.A. Kivelson, Phys. Rev. Lett. **99**, 247203 (2007).